Unsteady Laminar Boundary-Layer Separation on Oscillating Configurations

Wolfgang Geissler*
DFVLR, Göttingen, Federal Republic of Germany

A finite difference procedure has been developed to calculate unsteady two-dimensional laminar boundary layers on oscillating configurations. The method works in regions of reversed flow without numerical difficulties. The oscillating flat plate is investigated as a first test case to prove the validity and efficiency of the calculation procedure. The method is then applied to the more interesting case of an airfoil with pitching oscillations. Three incidence cases for the NACA 0012 airfoil are treated: $\alpha_0 = 0$, 8, and 16 deg with $\alpha_1 = 8$ deg oscillation amplitude and various reduced frequencies. Special emphasis is placed on the investigation of the flow behavior close to boundary-layer separation. The results of the unsteady boundary-layer calculation give the necessary input to model unsteady separated flows.

Introduction

In recent years, several successful methods have been developed[1,2] to calculate steady lift and drag on airfoils under stalled flow conditions. These methods use a combination of inviscid panel-type and boundary-layer calculation procedures to determine iteratively the separation points on the airfoil. Equivalent Kutta conditions are then applied at the separation points on the upper and lower surfaces. The separation and wake regions are modeled either by a displacement[1] or vortex sheet model.[2]

Additional problems occur, however, for airfoils in unsteady motion, as has been pointed out by Sears.[3] In Ref. 3 a relationship between velocities at instantaneous locations of the boundary-layer separation points and the overall unsteady circulation $\Gamma(t)$ is given by

$$\left[\frac{1}{2}U^2 - U_{sep}U\right]_B^A = -\frac{d\Gamma}{dt} \tag{1}$$

where $[\ ]_B^A$ refers to the difference between the upper and lower surface separation points. U is the velocity at the outer edge of the boundary layer and U_{sep} the velocity of the corresponding separation phenomenon along the wall. In steady flow, Eq. (1) simplifies to

$$[\tfrac{1}{2}U^2]_B^A = 0 \tag{2}$$

which has been used as the Kutta condition in steady calculation procedures. For unsteady nonseparated flow, the free vorticity strength $d\Gamma/dt$ leaves the wing at the trailing edge with $U_{sep} \equiv 0$ in Eq. (1). This special case has been treated in Ref. 4 for oscillating three-dimensional wings with a thin doublet sheet representing the wake.

To construct a corresponding model in the unsteady separated case, two quantities must be calculated:

1) The time-dependent velocities $U(t)$ at the instantaneous separation points.

2) The time-dependent movement of the separation points U_{sep} along the airfoil surface.

Both quantities are determined by the present unsteady boundary-layer calculation. The calculation procedure is a well-known Crank-Nicolson finite difference method which has already been applied to the calculation of steady three-dimensional boundary layers on blunt bodies.[5] Similar to the three-dimensional case, the determination of separation in unsteady flow is not straightforward. In the unsteady case, it is well known that reversed-flow regions occur along the surface with no sign of severe boundary-layer breakoff. The calculation procedure must, therefore, be able to handle backflow regions in unsteady flow. A suitable test case to prove the ability of the boundary-layer code is the oscillating flat plate oscillating in its own plane. This problem is well known in technical literature sources and was treated first by Lighthill.[6] Details of the calculation procedure and corresponding results are given in Ref. 7.

With a successful test for the flat plate, the method will then be applied to the more interesting and difficult case of an airfoil with pitching oscillations. This problem has also been treated in various investigations. In Ref. 8 the problem of dynamic stall is investigated by means of a finite difference procedure which solves the laminar and turbulent unsteady boundary layers. The calculation was stopped, however, at the position of zero skin friction as the usual steady separation criterion. In Ref. 9 the unsteady boundary-layer calculation was carried out on the basis of an integral method. The advantage of this method is its speed and sufficiency, but it is not appropriate to investigate the details of the boundary-layer development close to unsteady separation, specifically in the laminar case. In the present investigation, the laminar boundary-layer equations are transformed into a stagnation point fixed frame of reference. This has the advantage that the boundary-layer calculation can start at each time step from the instantaneous position of the stagnation point. Therefore, a rather complicated special treatment of the stagnation point region[10] is avoided.

For a successful treatment of boundary-layer problems, a detailed knowledge of boundary conditions and initial conditions is essential. The unsteady panel method described in Ref. 4 is able to calculate the necessary inviscid velocities on the real surface of the oscillating configuration. Presently, the outer boundary condition remains unchanged during the boundary-layer calculation. In a later step, the inviscid velocities should be allowed to adjust to the effect of the boundary-layer displacement in a strong interaction procedure.

Unsteady Boundary-Layer Equations—Finite Difference Procedure

The solution procedure has been applied to the well-known set of unsteady laminar boundary-layer equations expressing

Received Dec. 16, 1983; revision received April 18, 1984,

*Head of Unsteady Aerodynamics Branch, Institute of Aeroelasticity.

the conservation of mass and momentum[11]:

$$\frac{\partial u}{\partial x}+\frac{\partial \bar{v}}{\partial \bar{y}}=0 \tag{3}$$

$$\frac{\omega^*}{2\pi}\frac{\partial u}{\partial \bar{T}}+u\frac{\partial u}{\partial x}+\bar{v}\frac{\partial u}{\partial \bar{y}}=\frac{\omega^*}{2\pi}\frac{\partial U}{\partial \bar{T}}+U\frac{\partial U}{\partial x}+\frac{\partial^2 u}{\partial \bar{y}^2} \tag{4}$$

where x, y, and u, U, v are dimensionless with the reference length c and reference velocity U_∞, respectively. In addition, y and v have been stretched by $\sqrt{Re}$ ($Re = U_\infty c/\nu$, Reynolds number). Time t is made dimensionless and corresponds to the wavelength of the harmonic oscillation in the following manner:

$$T = t\cdot U_\infty/c \qquad \bar{T} = T/(2\pi/\omega^*) \tag{5}$$

with the reduced frequency

$$\omega^* = \omega\cdot c/U_\infty \tag{6}$$

The corresponding boundary conditions are

$$u=\bar{v}=0 \quad \text{for} \quad \bar{y}=0$$
$$u=U \quad \text{for} \quad \bar{y}\to\infty \tag{7}$$

Numerical calculation of the set of Eqs. (3) and (4) is carried out by a Crank-Nicolson type of finite difference procedure, which was first applied by Hall.[12] The implicit formulation normal to the wall ($\bar{y}$ direction) leads to a linear system of equations with a tridiagonal coefficient matrix, which can be solved by standard means. Continuity as well as momentum equations are solved by iteration starting with linear extrapolated values. The calculation is continued until the differences of the u-velocity components between two cycles are less than a prescribed tolerance.

The calculation progresses first in the x-direction with constant mesh sizes Δx and then continues at the next time level at $\bar{T} = \bar{T} + \Delta T$ with constant time steps $\Delta\bar{T}$. The growth of the boundary layer is taken into account by adding additional mesh points in the $\bar{y}$ direction. If the number of mesh points in this direction exceeds 100, the mesh size $\Delta\bar{y}$ is doubled.

The ratio of mesh sizes $\Delta x/\Delta T$ determines the limit of the numerical calculation due to the CFD stability condition. This limit may be obtained in regions of reversed flow. The stability condition is proved during the entire calculation.

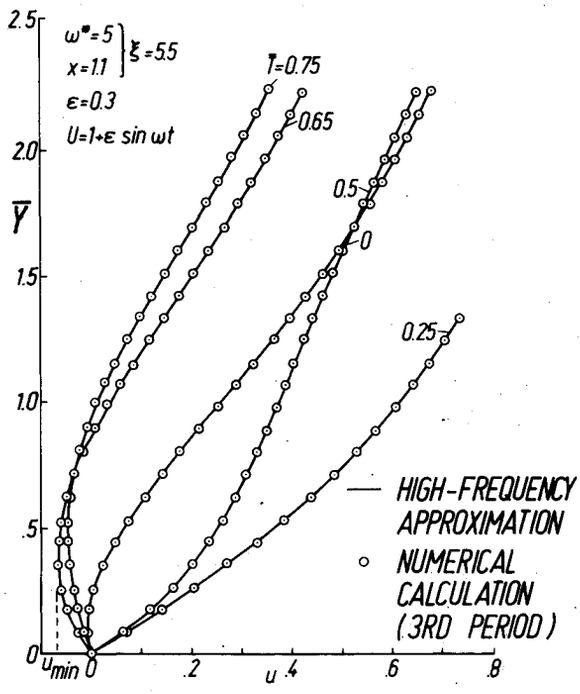

Fig. 1 Boundary-layer profiles on oscillating flat plate.

Oscillating Flat Plate

The numerical procedure was first applied to the case of a flat plate oscillating in its own plane.[6] In this case the outer inviscid velocity is determined by

$$U(t) = U_\infty(1+\epsilon e^{i\omega^* T}) \tag{8}$$

with ϵ as the amplitude of oscillation. For low and high values of the unsteady parameter $\xi = x\cdot\omega^*$, corresponding low- and high-frequency solutions can be developed based on ordinary differential equations. A comparison of these approximations with the results of the numerical calculation provides an excellent check of the validity of the finite difference procedure. Figure 1 shows velocity profiles for the cases of $\xi = 5.5$ and $\epsilon = 0.3$. The solid lines are results from the high-frequency solution. The circles are obtained from numerical calculation after three time periods; correspondence is excellent. Figure 1 shows that backflow occurs further on over a part of the oscillatory cycle. The numerical calculation moves through the reversed-flow region without difficulties. It is pointed out in Ref. 6, however, that the calculation breaks down if the amplitude ϵ is increased such that backflow reaches the leading edge of the plate.

Airfoil in Pitching Motion

With a successful check of the finite difference procedure to solve the unsteady boundary-layer equations even in regions

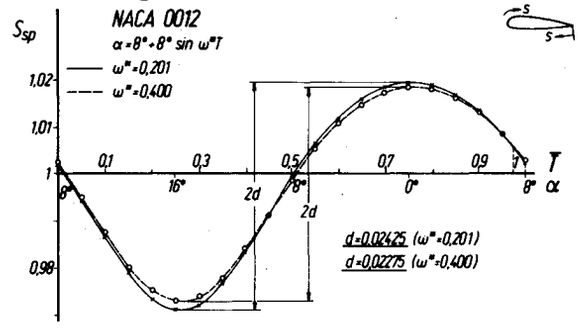

Fig. 2a Displacement of stagnation point at the nose of an oscillating airfoil.

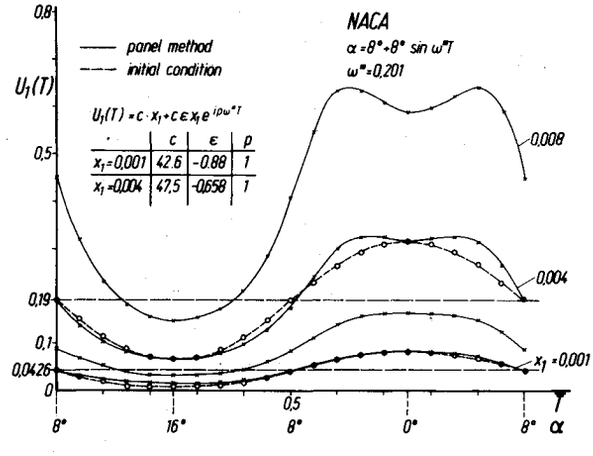

Fig. 2b Inviscid velocities close to stagnation point. Best fit for initial conditions in time domain.

of reversed flow, the airfoil in pitching motion can be investigated as a problem of more practical interest. The NACA 0012 airfoil has been chosen as a test case.

Outer Inviscid Flow (Panel Method)

In Ref. 4 a panel method is described to calculate the steady as well as unsteady inviscid flows about three-dimensional oscillating wings. A combination of sources and doublets on the wing surface, as well as a doublet sheet representing the wake, has been used to calculate velocities and pressures on the real body surface. Velocities in a streamwise section close to the wing symmetry plane as obtained by the panel method are assumed as outer boundary conditions. Although the method is linear in amplitude, the results are applied also to moderate- and high-amplitude oscillations common in dynamic stall problems.

Stagnation Point Fixed Frame of Reference

In the flat-plate case, the numerical calculation always starts at the plate leading edge. The front stagnation point on profiles, which usually serves as the starting point in steady boundary-layer calculations, is moving in the unsteady case.

Figure 2 shows the instantaneous positions of the stagnation point for the incidence variation

$$\alpha = 8 \text{ deg} + 8 \text{ deg} \sin \omega^* T$$

and the two reduced frequencies $\omega^* = 0.2$ and 0.4. The movement of the stagnation point is nearly harmonic and 180 deg out of phase relative to α. The effect of reduced frequency ω^* is small. To start the unsteady boundary-layer calculation from the instantaneous positions of the stagnation point, a stagnation point fixed frame of reference has been chosen (Index 1)

$$x_{1U} = x - x_0 + de^{i\omega^* T} \quad \text{(upper surface)}$$

$$x_{1l} = -(x - x_0) - de^{i\omega^* T} \quad \text{(lower surface)} \tag{9}$$

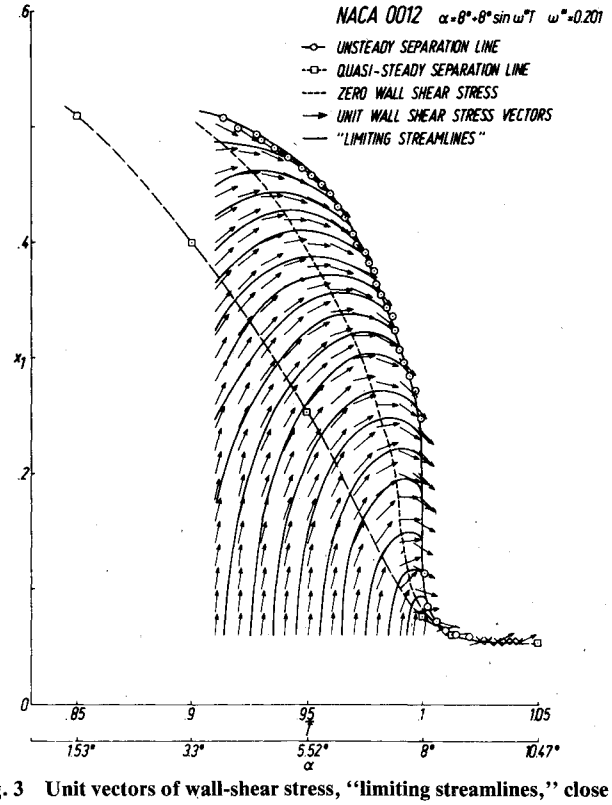

Fig. 3 Unit vectors of wall-shear stress, "limiting streamlines," close to separation.

with x_0 as the steady mean position of the stagnation point and d as the amplitude of movement. With

$$U_{1\text{kin}} = \frac{\partial x_1}{\partial t} = \pm i\omega^* de^{i\omega^* T} \tag{10}$$

as the kinematic velocity of the stagnation point, the velocities in the boundary layer are changed:

$$u_1 = u + U_{1\text{kin}} \qquad v_1 = \tilde{v} \tag{11}$$

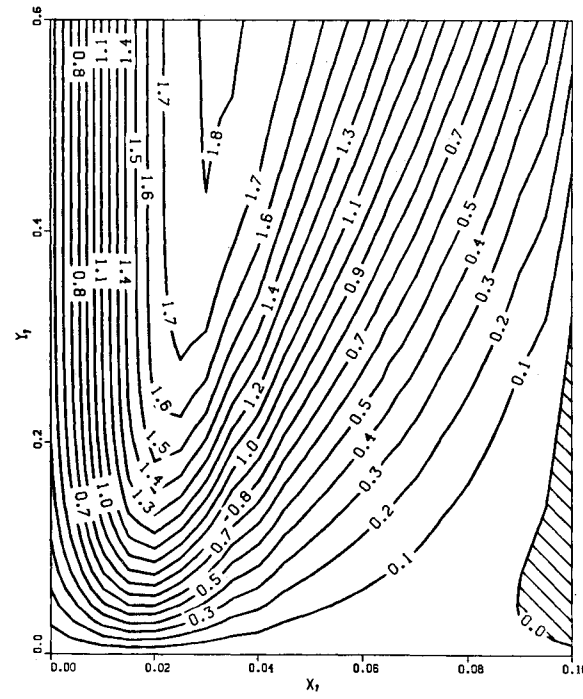

Fig. 4a Contour plots of velocity component u_1 in the boundary layer close to separation. $\bar{T} = 1.002$, $\alpha = 8.1$ deg$\uparrow$ ($\alpha = 8$ deg $+ 8$ deg $\cdot \sin \omega^* T$, $\omega^* = 0.2$).

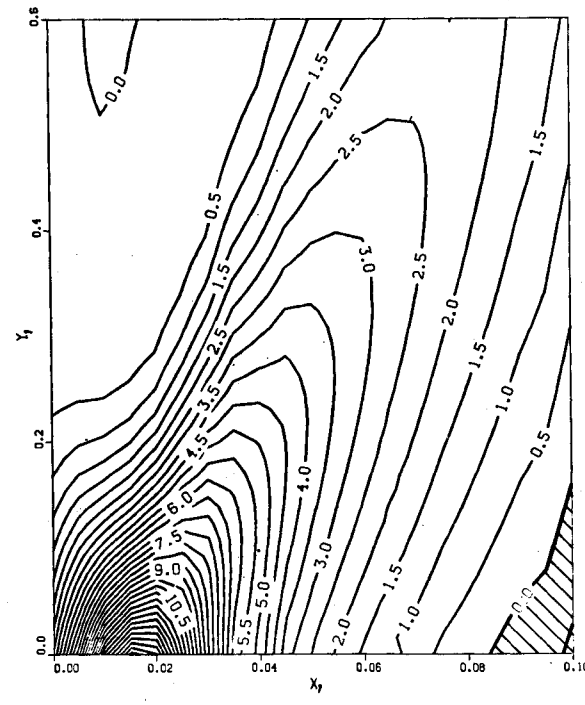

Fig. 4b Contour plots of vorticity in the boundary layer close to separation. $\bar{T} = 1.002$, $\alpha = 8.1$ deg$\uparrow$ ($\alpha = 8$ deg $+ 8$ deg $\cdot \sin \omega^* T$, $\omega^* = 0.2$).

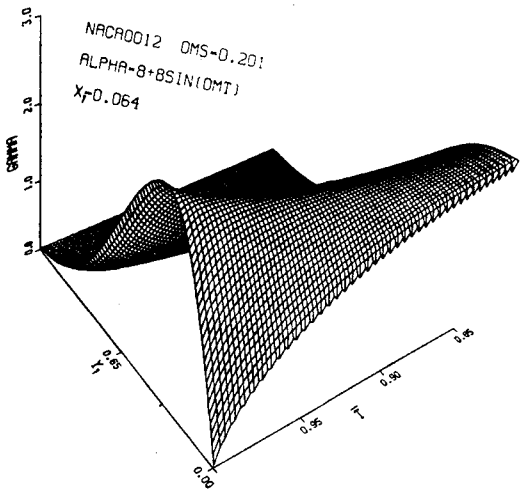

Fig. 5a Vorticity distribution close to separation at $x_1 = 0.064$, $0.85 \leq \bar{T} \leq 1$, and $1.53 \leq \alpha \leq 8$ deg.

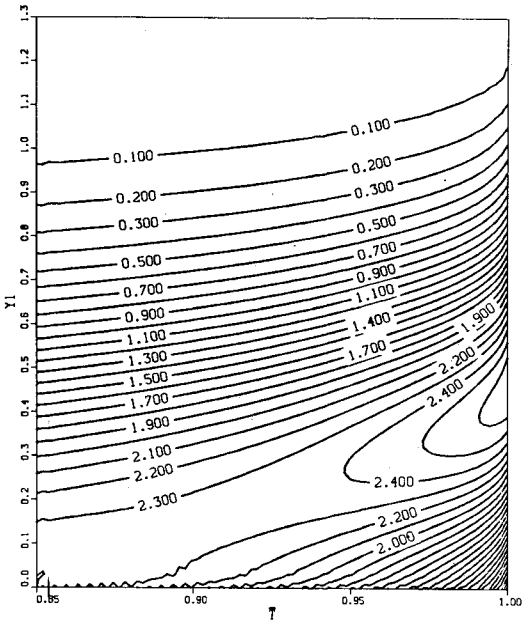

Fig. 5b Vorticity contours close to separation at $x_1 = 0.064$, $0.85 \leq \bar{T} \leq 1$, and $1.53 \leq \alpha \leq 8$ deg.

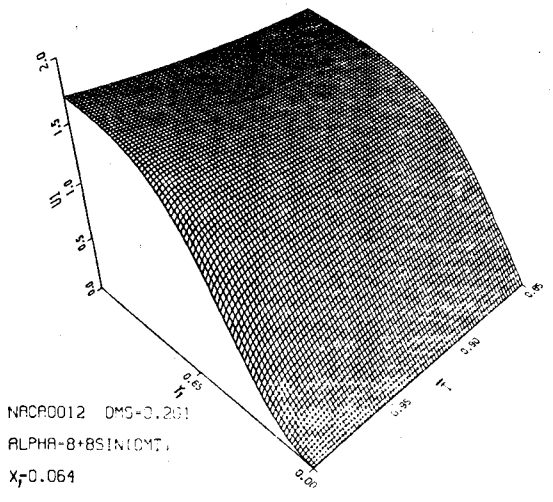

Fig. 5c Distribution of velocity component u_1 $0.85 \leq T \leq 1$, and $1.52 \leq \alpha \leq 8$ deg.

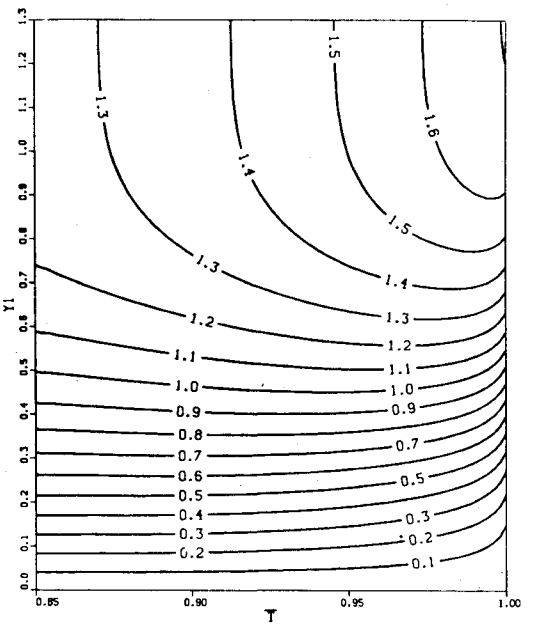

Fig. 5d Velocity contours, $0.85 \leq \bar{T} \leq 1$ and $1.52 \leq \alpha \leq 8$ deg.

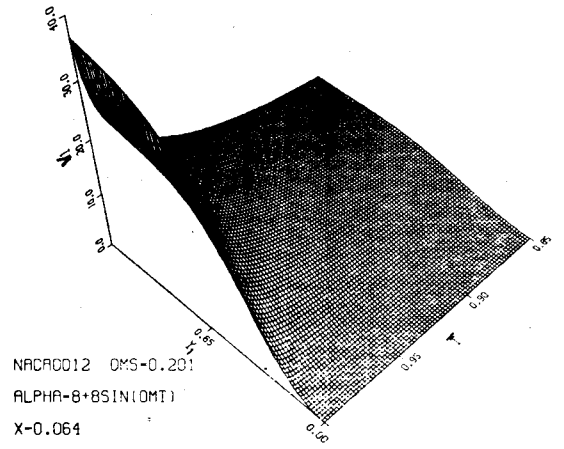

Fig. 5e Normal velocity distribution contours, $0.85 \leq \bar{T} \leq 1$ and $1.53 \leq \alpha \leq 8$ deg.

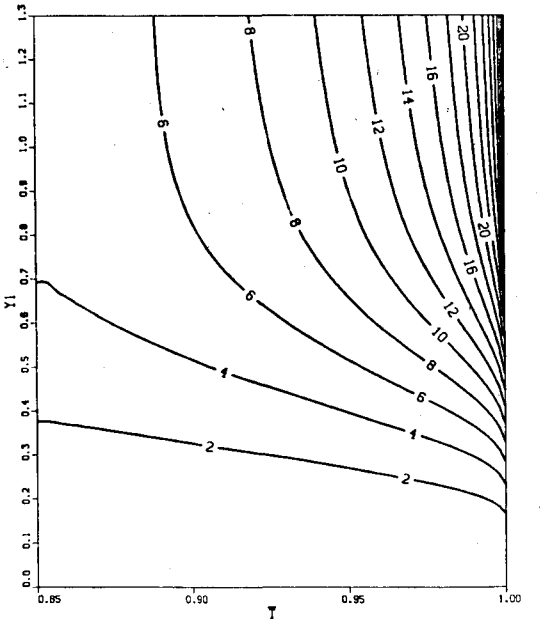

Fig. 5f Normal velocity contours, $0.85 \leq \bar{T} \leq 1$ and $1.53 \leq \alpha \leq 8$ deg.

Substitution of Eq. (9) into Eqs. (3) and (4) yields no formal difference in the boundary-layer equations. The boundary conditions, however, change to

$$y_1 = 0: \quad u_1 = \pm U_{1\text{kin}} = \pm i\omega^* d e^{i\omega^* T}$$

$$y_1 \to \infty: \quad u_1 = U[x_1(x,t),t] \pm U_{1\text{kin}} = U_1 \pm i\omega^* d e^{i\omega^* T} \qquad (12)$$

The $\pm$ signs refer to the upper and lower surfaces, respectively. Numerical calculation is now carried out in the system x_1, y_1 with u_1, U_1, v_1, etc.

Initial Conditions

To start the calculation, appropriate initial conditions must be specified. A linearly varying inviscid velocity $U_1(x_1, T)$ is assumed close to the stagnation point

$$U_1 = cx_1 + c\epsilon x_1 e^{ip\omega^* T} \qquad (13)$$

with x_1 as the distance from the stagnation point. The parameters c, ϵ, and p have to be determined such that a good fit is obtained with the U_1 distribution calculated from the panel method. Figure 2b shows $U_1(T)$ distributions from the panel method (solid lines) and the corresponding curve fit due to Eq. (13) (dashed lines) at the two positions $x_1 = 0.001$ and 0.004. The correponding parameters for the two cases (c, ϵ, and p) appear in the figure. It has been shown in Ref. 13 that, with the outer boundary condition (13), the boundary-layer equations can be reduced to a set of ordinary differential equations solved by the Runge-Kutta method. The results are initial boundary-layer profiles at x_1 for all $\bar{T}$. Initial conditions at $\bar{T} = \bar{T}_0$ for all x_1 can be specified by the numerical solution of the steady boundary-layer equations, taking into account the instantaneous inviscid velocities at $\bar{T} = \bar{T}_0$.

Results

Three incidence cases have been investigated in detail for the NACA 0012 airfoil section[14]:

1) $\alpha = 0$ deg + 8 deg sin$\omega^* T$
2) $\alpha = 8$ deg + 8 deg sin$\omega^* T$
3) $\alpha = 16$ deg + 8 deg sin$\omega^* T$

If the numerical calculation is carried out over the entire $x_1, \bar{T}$ domain, regions of reversed flow are reached through which the calculation can first be continued up to a point where the calculation comes to a breakdown. The question arises whether this breakdown has a pure numerical cause or whether it is due to the specific behavior of boundary-layer quantities. In the following sequence of figures, it will be shown that both causes are involved.

First, for case 2 above, Fig. 3 shows unit vectors of wall-shear stress in the $x_1, \bar{T}$ domain close to breakdown. To define a "direction" in the $x_1, \bar{T}$ domain, a step τ_w in the x_1 direction is combined with an always constant step in the $\bar{T}$ direction. Therefore, a horizontal vector indicates zero wall-shear stress. Between the dashed line and the solid boundary the flow is reversed. The solid boundary is interpreted as the location of the unsteady separation phenomenon. It can be seen in Fig. 3 that the separation velocity is strongly increased if the separation point is moving upstream. Integrating the wall-shear stress vectors, the equivalence of wall streamlines is determined and indicated in Fig. 3. Similar plots have also been presented in Ref. 15. Although these "streamlines" have no direct physical meaning, their behavior in the vicinity of unsteady boundary-layer breakdown is very similar to three-dimensional steady flow. As in the steady case,[5] the solid boundary seems to be the envelope of limiting streamlines. The advantage of a vector plot similar to Fig. 3 is that the distinctions between downstream-directed flow and reversed flow can be made at once. The important fact is that the "limiting streamlines," simply obtained by integrating the vector field, show a characteristic strong curvature close to the

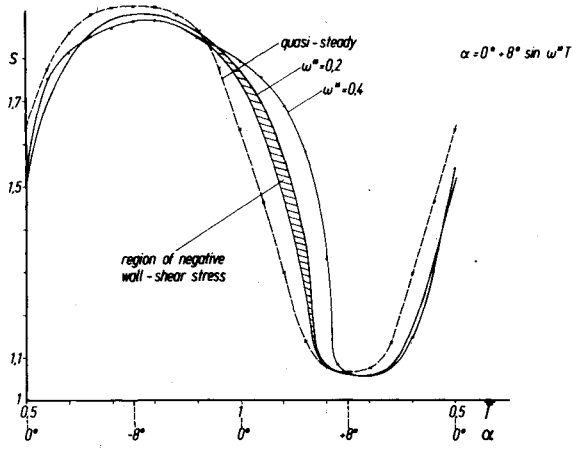

a) 0 deg mean incidence.

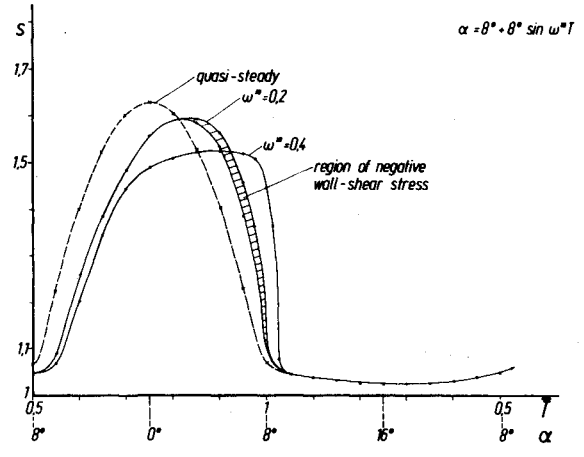

b) 8 deg mean incidence.

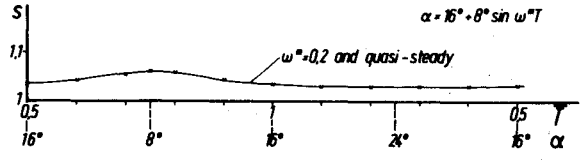

c) 16 deg mean incidence.

Fig. 6 Quasisteady and unsteady separation lines over a period of oscillations.

breakdown of the boundary-layer calculation. This may be one indication of unsteady separation, as has also been pointed out in Ref. 15. As opposed to steady boundary-layer flows, where separation occurs at the position of zero wall shear, the position of boundary-layer separation in unsteady flow is shifted downstream beyond the point of zero wall shear. This typical unsteady flow behavior makes it difficult to define a precise separation criterion. Figure 3 gives only a relatively weak criterion for unsteady separation. It will be outlined in the following section that the specific behavior of boundary-layer quantities such as vorticity and velocity components, specifically the normal velocity component, give a stronger (but also imprecise) separation criterion.

Another indicator of unsteady separation is known as the Moore, Rott, and Sears criterion described in Ref. 16, where separation occurs at the point where the shear vanishes at a stagnation point within the flow. This criterion can be investigated in a coordinate system fixed to the moving separation point. No attempt has been made so far in the present

study to investigate the latter criterion. This is also complicated by the fact that a moving (stagnation point fixed) frame of reference has previously been used. Figure 3 shows only a small part of the calculation domain, which will be presented later in its entirety.

Figures 4 and 5 show typical details of flow quantities inside the boundary layer. Figure 4a gives the contour lines of the tangential velocities and Fig. 4b gives the corresponding contour lines of vorticity. The right-hand margin of these figures corresponds to the last mesh point before breakdown. A region of reversed flow and negative vorticity is typical within this area. Tongues of equal vorticity lines are pointing outside (Fig. 4b). Figure 5 shows vorticity, tangential and normal velocities inside the boundary layer at a specific x_I position along $\bar{T}$. The positions can be specified as in Fig. 3. Figure 5a indicates that vorticity is spreading outside into the fluid with increasing time. The corresponding contour lines (Fig. 5b) become steeper close to breakdown. The tangential velocities (Fig. 5c) show a point of inflection and a small backflow region close to the wall. Finally, Figs. 5e and 5f give the behavior of the normal velocity. The increasing steepness of v_I in the outer region of the boundary layer (Fig. 5e) is severe. This increasing steepness is interpreted as the reason for the breakdown of the numerical calculation procedure.

Continuation of the numerical method poses no problem as long as the separation point moves upstream. Difficulties occur, however, in regions of reattachment due to a lack of information from previous time levels. To follow approximately the reattachment line, the calculation was continued at a specific $\bar{T}$ level on a quasisteady basis. Figure 6 shows the separation lines for the three incidence cases 1-3 above over the entire $s,\bar{T}$ domain, where s is the original surface coordinate of the profile after retransformation from the stagnation point fixed frame. In Figs. 6a and 6b the three cases $\omega^* = 0$ (quasisteady), 0.2, and 0.4 are indicated. The curves show the same behavior which has been found qualitatively in water tunnel experiments.[17] In the highest incidence case 3 (Fig. 6c), the separation line is located very close to the leading edge over the entire cycle of oscillation. In this case there is a very severe production and shedding of vorticity into the boundary layer.[14]

From Fig. 6 the necessary information can be specified on the Sears criterion, Eq. (1); namely, the velocity of the unsteady separation phenomenon U_{sep}, as well as the velocity U at separation. These quantities could then be used as input for an interactive unsteady viscous/inviscid flow model.

Conclusion

A finite difference method has been developed to calculate unsteady laminar boundary layers on oscillating configurations. The method has the capability to handle reversed-flow regions. It was tested for the oscillating flat plate and then applied to the NACA 0012 airfoil section at high-amplitude pitching oscillations about various mean incidences and for different reduced frequencies. Details of the flow behavior close to separation are investigated. Separation and reattachment lines over the entire $s,\bar{T}$ domain are calculated. These results give the necessary input for an unsteady viscous/inviscid flow model.

Acknowledgments

The main parts of this investigation were carried out while the author was on a one-year leave at the NASA Ames Research Center, Moffett Field, Calif. The use of the Ames computer facilities under the auspices of the Aerodynamic Research Branch is gratefully acknowledged.

References

[1] Jakob, K., "Advancement of a Method for Calculating Separated Flows around Airfoils with Special Consideration of Profile Drag," DFVLR, Göttingen, DLR-FB 76-36, 1976; translated as ESA-TT-373, April 1977.

[2] Maskew, B. and Dvorak, F.A., "The Prediction of C_{LMAX} Using a Separation Flow Model," *Journal of the American Helicopter Society,* Vol. 23, April 1978, pp. 2-8.

[3] Sears, W.R., "Unsteady Motion of Airfoils with Boundary-Layer Separation," *AIAA Journal,* Vol. 14, Feb. 1976, pp. 216-220.

[4] Geissler, W., "Nonlinear Unsteady Potential Flow Calculations for Three-Dimensional Oscillating Wings," *AIAA Journal,* Vol. 16, Nov. 1978, pp. 1168-1174.

[5] Geissler, W., "Three-Dimensional Laminar Boundary Layer over a Body of Revolution at Incidence and with Separation," *AIAA Journal,* Vol. 12, Dec. 1974, pp. 1743-1745.

[6] Lighthill, M.J., "The Response of Laminar Skin Friction and Heat Transfer Fluctuations in the Stream Velocity," *Proceedings of the Royal Society,* Ser. A, No. 224, 1954, pp. 1-23.

[7] Geissler, W., "Unsteady Laminar Boundary Layer Calculations on Oscillating Configurations including Backflow. Part I: Flat Plate Oscillating in Its Own Plane," NASA TM 84319, March 1983.

[8] McCroskey, W.J. and Philippe, J.J., "Unsteady Viscous Flow on Oscillating Airfoils," *AIAA Journal,* Vol. 13, Jan. 1975, pp. 71-79.

[9] Consteix, J. and Houdville, R., "Singularities in Three-Dimensional Turbulent Boundary Layer Calculations and Separation Phenomena," *AIAA Journal,* Vol. 19, Aug. 1981, pp. 976-985.

[10] Cebeci, T. and Carr, L.W., "Prediction of Boundary Layer Characteristics on an Oscillating Airfoil," NASA TM 81 303, July 1981, also; *Unsteady Turbulent Shearflows*, edited by R. Michel, J. Cousteix, R. Houndville, Toulouse, France, 1981, pp. 185-196.

[11] Schlichting, H., *Boundary-Layer Theory*, 7th Ed., McGraw-Hill Book Co., New York, 1979.

[12] Hall, M.G., "A Numerical Method for Calculating Unsteady Two-Dimensional Laminar Boundary Layers," *Ingenieur Archiv,* Vol. 38, Aug. 1969, pp. 97-106.

[13] Glauert, M.B., "The Laminar Boundary Layer on Oscillating Plates and Cylinders," *Journal of Fluid Mechanics,* Vol. 1, 1965, pp. 97-110.

[14] Geissler, W., "Unsteady Laminar Boundary Layer Calculations on Oscillating Configurations Including Backflow. Part II: Airfoil in High Amplitude Pitching Motion—Dynamic Stall," NASA TM 84319, March 1983.

[15] Wang, K.C., "On the Current Controversy of Unsteady Separation," *Proceedings of the Symposium on Numerical and Physical Aspects of Aerodynamic Flow,* California State University, Long Beach, Calif. 1981.

[16] Telionis, D.P., "Unsteady Viscous Flows," *Springer Series in Computational Physics,*" Springer-Verlag, New York, 1981.

[17] McAllister, K.W., and Carr, L.W. "Water Tunnel Visualizations of Dynamic Stall," *Journal of Fluids Engineering,* Vol. 101, Sept. 1979, pp. 376-380.